22nd International Conference on Information Fusion
Ottawa, Canada - July 2-5, 2019

Probability Distribution for Association of Maneuvering Vehicles

Brita H. H. Gade
FFI (Norwegian Defence Research Establishment)
Kjeller, Norway
Brita.Gade@FFI.no

Carina N. Vooren
FFI (Norwegian Defence Research Establishment)
Kjeller, Norway
Carina-Norberg.Vooren@FFI.no

Morten Kloster
FFI (Norwegian Defence Research Establishment)
Kjeller, Norway
Morten.Kloster@FFI.no

***Abstract*—The usual multivariate Gaussian probability may not give a good representation of the real measurement to track association probability if the time period of the prediction is long compared to the time scales of vehicle turning maneuvers. This paper proposes a fast procedure for calculating a more correct measurement to track association probability in such cases.**

Keywords—association, probability distribution, target tracking

I. Introduction

In target tracking, association is needed if the scene contains more than one target or if the sensor(s) may give false measurements (also called false alarms or clutter). Most association schemes need a way to determine the probability that a certain measurement belongs to a certain track.

Many association methods such as SNN (Suboptimal Nearest Neighbour) and GNN (Global Nearest Neighbour) [1] solve the association problem by, for each track-measurement pair, using a cost of assigning the measurement to the track. The simplest approach is to use a cost based on the Euclidian distance between the predicted track position and the measurement. For models described by multivariate Gaussian probabilities, one can use a cost equal to the Mahalanobis distance [2], where the uncertainty of both the predicted track position and of the measurement, as given by their covariance matrices, are used in the calculation.

Other association methods, such as HOMHT (Hypothesis Oriented Multiple Hypothesis Tracking) [3], use the multivariate Gaussian probability directly.

The use of multivariate, usually 2D or 3D, Gaussian probability works well for vehicles with little turning maneuvers between measurements. If the time period between two measurements is long compared to the time scales of the vehicle turning maneuvers, however, the multivariate Gaussian probability does not give a good representation of the possible future vehicle positions. This is illustrated in Fig.1, where a measurement belonging to airplane A will have a very low Gaussian probability to belong to airplane A. Even though the measurement is far from the real probable positions of airplane B, it will have a relatively high Gaussian probability of belonging to airplane B. It will thus be assumed to belong to airplane B, and not to airplane A, if a multivariate Gaussian probability is used.

Within gating, solutions for handling maneuvering targets have been studied by [4], who present four gating techniques for IMM-PDA (Interacting Multiple Model – Probabilistic Data Association), all based on ellipsoid gates, and more thoroughly by [5] who generalize the theory of validation gating for non-linear and non-Gaussian systems, but whose method is assumed to be too computationally intensive for implementation. A fast validation region with a gate probability close to 1 is presented in [6].

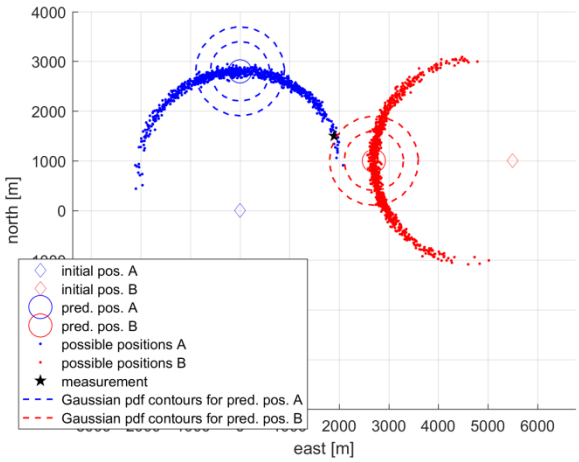

Fig. 1. Two airplanes A (blue) and B (red), with 1000 different simulated end positions, where the initial velocity used is s_0=280 m/s and the timeperiod is Δt=10s

Non-Gaussian pdf contours have been studied within the field of robotics, where Gaussian pdfs evolve into banana-shaped figures due to e.g. noisy wheel speeds [7], [8], [9]. We have not found good alternatives to the multivariate Gaussian probability for use in HOMHT and other methods that use the probability density level for association. The aim of this paper is to give such an alternative, with little extra computational cost.

Section II presents the notation and assumptions of the paper and shows possible future positions for a maneuvering vehicle. Section III deduces the corresponding Constant Acceleration and Turn rate (CAT) distribution and section IV shows the procedure for finding the probability density of associating the vehicle track to a received measurement. Section V compares the proposed CAT distribution to different multivariate Gaussian distributions for a maneuvering airplane trajectory. Section VI gives recommendations about when to use or not use the CAT distribution.

II. Notation and Motivation

In this paper we have made the following assumptions:

- Between each measurement, the vehicle trajectory has a constant unknown turn rate $\omega \sim N(0,\sigma_\omega)$ and a constant unknown acceleration $a \sim N(0,\sigma_a)$. This is a more general assumption than the ordinary assumption of constant speed and course, with acceleration modeled as noise.

978-0-9964527-8-6

- We assume the measurement noise to be very small compared to the uncertainty of the future vehicle position, i.e. we assume the process noise covariance to be much larger than the measurement noise covariance. This is usually true for air surveillance and for maritime surveillance with satellite-mounted sensors.
- We also consider the uncertainty of the initial velocity estimate to be very small.

The vector from the updated position at time k to the new measurement at time k+1 is in this paper decomposed to the across-track component x and the along-track component y.

Fig. 2 shows 10000 points where each point is drawn from a Gaussian distribution with σ_a=1.67 m/s^2 and σ_ω=3.33 deg/s.

Fig. 3 shows the end positions, represented by x and y, that results from simulating each point in Fig. 2 as a vehicle with initial velocity s_0=280 m/s for a time period Δt=15s between the initial position and the new measurement. Instead of performing actual simulations, the points in Fig. 3 can also be found by inserting the values for each point from Fig. 2 into (9) in Appendix. A.

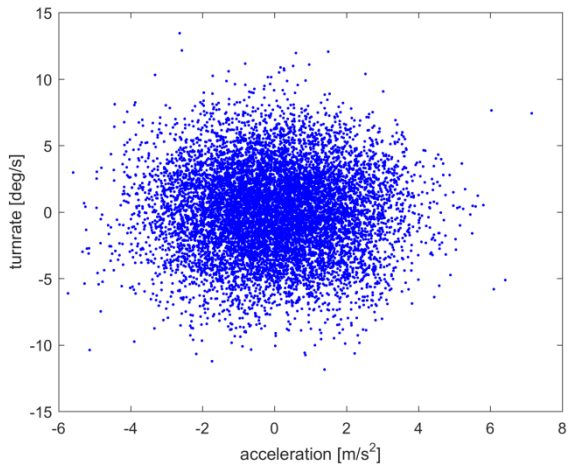

Fig. 2. 10000 points where each point is drawn from a Gaussian distribution with σ_a= 1.67 m/s^2 and σ_ω=3.33 deg/s

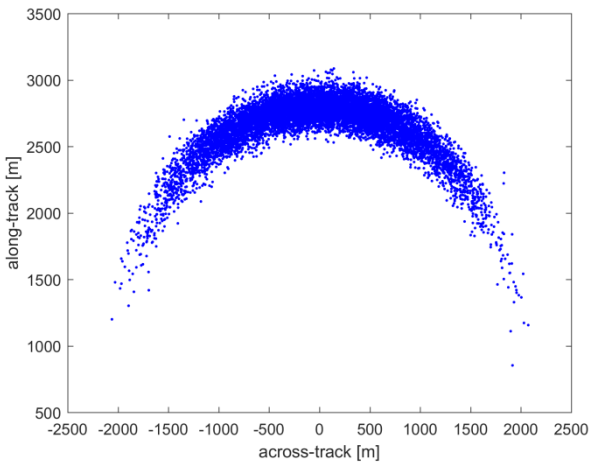

Fig. 3. End positions that results from simulating each point in Fig. 1 as a vehicle with initial velocity s_0=280 m/s, with a timeperiod Δt=15s between the updated position and the new measurement

From Fig. 3 it is clear that the distribution of the resulting positions cannot be represented in a good way by a multivariate Gaussian distribution in Cartesian coordinates. We need a new way to find the measurement to track association probability for maneuvering vehicles. We therefore aim at finding the probability distribution of the points in Fig. 3.

III. Probability Density

The probability density in the acceleration versus turn rate coordinate system is shown in Fig. 4 for σ_a = 1.67 m/s^2 and σ_ω = 3.33 deg/s. This is the probability distribution of the points in Fig. 2.

To be able to use the information from Fig. 4 to find the distribution of the points in Fig. 3, we first need to find the corresponding a and ω for each position given by x and y.

We have not found a closed-form solution that calculates a and ω from x and y, but Appendix B shows a fast iterated procedure to find a and ω from x and y.

Since we assume a and ω to be independently distributed, their distribution is given by

$$p(a,\omega) = \frac{1}{\sigma_a \sigma_\omega 2\pi} exp\left(-\frac{1}{2}\left(\frac{a^2}{\sigma_a} + \frac{\omega^2}{\sigma_\omega}\right)\right). \quad (1)$$

For an infinitesimal part of the area under the distribution, we have

$$dxdy = \det(\boldsymbol{J}) \cdot dad\omega, \quad (2)$$

where $\boldsymbol{J}$ is the Jacobi matrix:

$$\boldsymbol{J} = \begin{bmatrix} \frac{\partial y}{\partial a} & \frac{\partial y}{\partial \omega} \\ \frac{\partial x}{\partial a} & \frac{\partial x}{\partial \omega} \end{bmatrix}. \quad (3)$$

The equations for the elements of the Jacobi matrix can be found in Appendix C.

Since the volume under any infinitesimal part of the distribution should be equal for $p(a,\omega)$ and for the

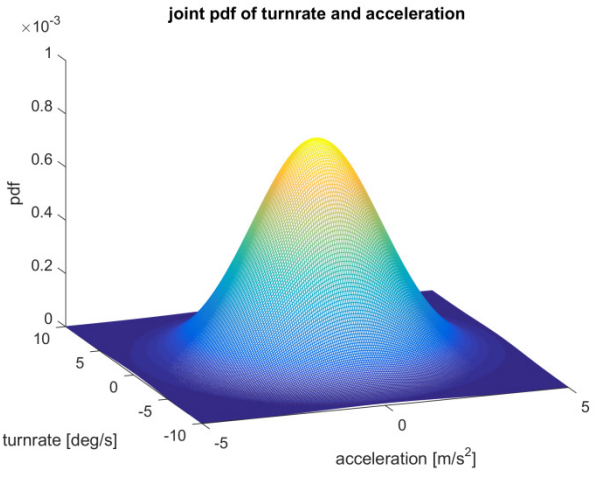

Fig. 4. Multivariate Gaussian distribution in the acceleration versus turn rate coordinate system with σ_a=1.67 m/s^2 and σ_ω=3.33 deg/s

corresponding $p(x,y)$, we have

$$p(x,y)\,dxdy = p(a,\omega)\,da d\omega. \quad (4)$$

By combining (2) and (4), we find that

$$p(x,y) = p(a,\omega)/\det(\boldsymbol{J}). \quad (5)$$

Fig. 5 shows the result of using (5) to calculate $p(x,y)$ for a tight grid of points. The parametres used are s_0=280 m/s, Δt=10 s, σ_a=1.67 m/s^2 and σ_ω=5 deg/s. This is the CAT probability distribution of the points in Fig. 3.

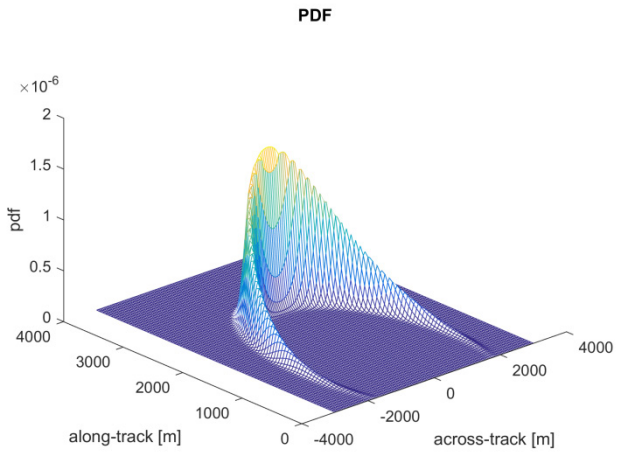

Fig. 5. The distribution $p(x,y)$ for a tight grid of points, where the parametres used are s_0=280 m/s, Δt=10 s, σ_a=1.67 m/s^2 and σ_ω=5 deg/s

IV. Procedure

The full procedure is illustrated in Fig. 6, where the following steps are marked with red numbers:

1. Use the measurement and the velocity vector direction to calculate x and y. For measurements received as latitude and longitude, this can easily be done by the use of n-vector [10].
2. Use the procedure from App. B to calculate a and ω.
3. Use (1) to find the pdf of the point (a,ω)
4. Use (5) to find the pdf of the point (x,y)

V. Results

We have tested the procedure shown in Fig 6. for the vehicle trajectory shown in Fig 7. This trajectory consists of several long, straight runs separated by sharp turns, and is thus not a close match to our statistical model. The vehicle speed is approximately 280 m/s, the maximum along-track acceleration is 5 m/s^2 and the time between each measurement is 10 s.

A. Distributions

We have tested 6 different distributions:

- CAT1: The CAT distribution with σ_a=5 m/s^2 and σ_ω=3.33 deg/s
- CAT2: Equal to CAT1, except that σ_ω=5 deg/s
- Gauss1: Multivariate Gaussian distribution with $\sigma_x = \sigma_y$ =100 m

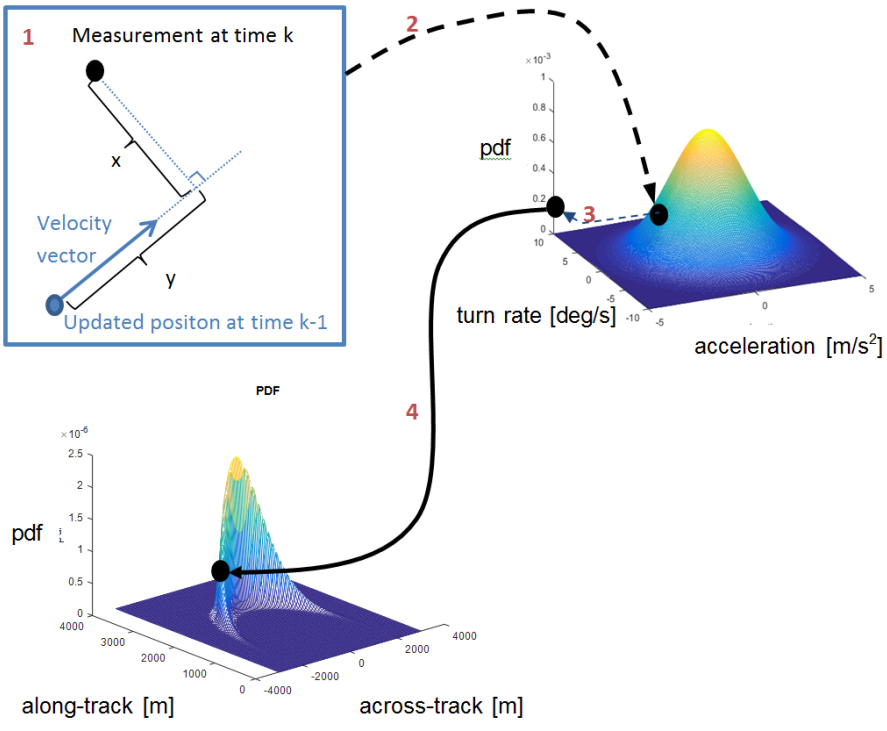

Fig. 6. Full procedure to find the CAT pdf from the measurement

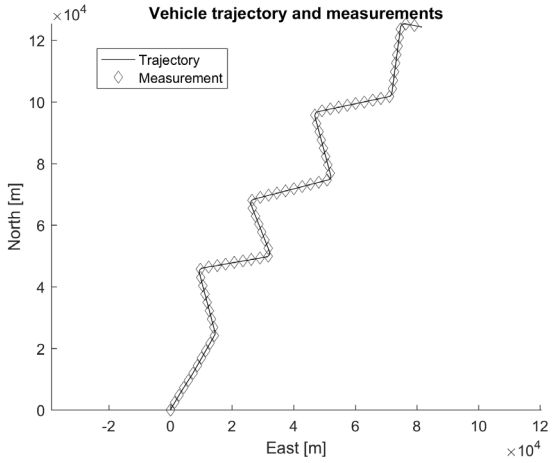

Fig. 7. Vehicle trajectory and measurements

- Gauss2: Multivariate Gaussian distribution with σ_x = 500 m and σ_y =100 m
- Gauss3: Multivariate Gaussian distribution with σ_x= 1000 m and σ_y = 200 m
- Gauss4: Distribution according to covariance matrix $\boldsymbol{C}$, made from the N=70 measurements shown in Fig. 7, where

$$\boldsymbol{C} = \frac{1}{N}\sum_{i=1}^{N}\begin{bmatrix} m_{x,i} \\ m_{y,i} \end{bmatrix}\begin{bmatrix} m_{x,i} - \bar{m}_{x,i} & m_{y,i} - \bar{m}_{y,i} \end{bmatrix} \quad (6)$$

where measurement i is given by $[m_{x,i}\ \ m_{y,i}]$ and the predicted position is given by $[\bar{m}_{x,i}\ \ \bar{m}_{y,i}]$.

Different combinations of the CAT and the Gaussian distributions are shown in Fig. 8.

B. Results along the vehicle trajectory

Fig. 9 shows the probability density for each measurement for each distribution. It shows that all distributions have higher pdf for measurements along the straight line segments of the vehicle trajectory, and much lower pdf for measurements during turns. Fig. 10 shows the same results, but with a logarithmic y axis. Here, the

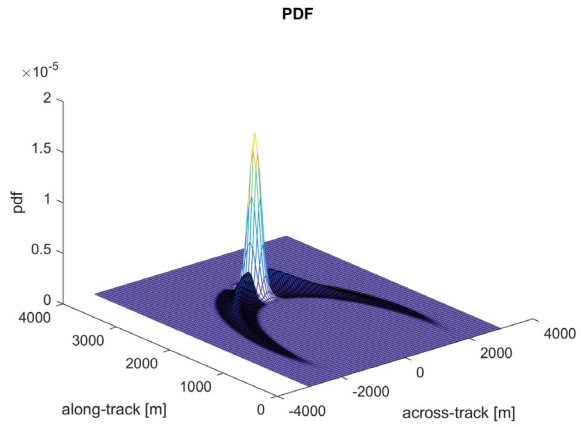

(a) CAT1 together with Gauss1

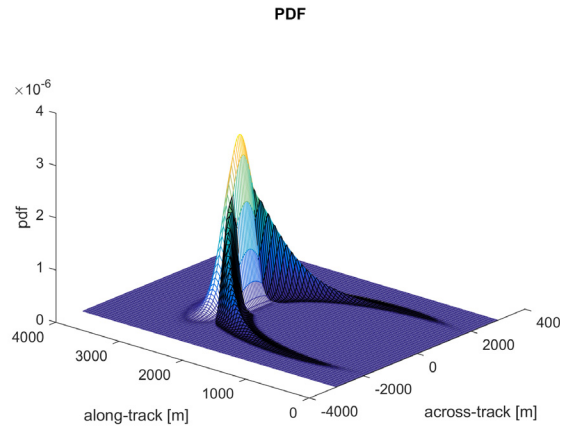

(b) CAT1 together with Gauss2

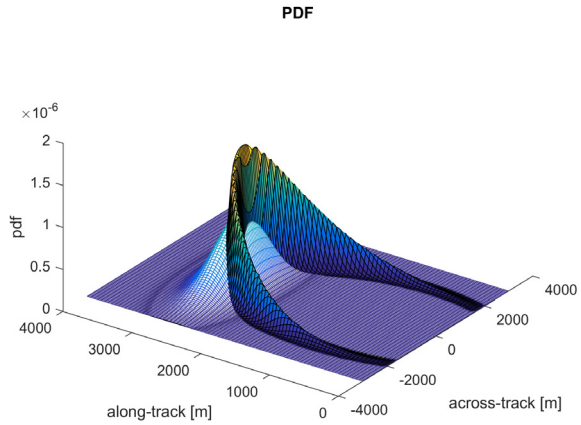

(c) CAT2 together with Gauss3

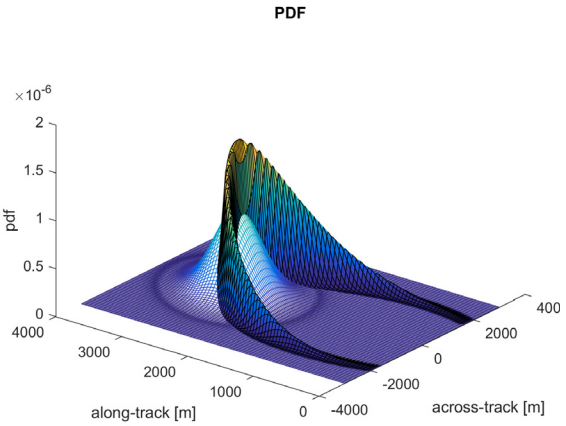

(d) CAT2 together with Gauss4

Fig. 8. Different combinations of the CAT and the Gaussian distributions

difference in the pdf during turns is much easier to distinguish. The difference is even easier to distinguish in Fig.11, which shows log10(pdf) and also has a logarithmic y axis. Here, it can easily be seen that all the Gaussian distributions have some very low estimated probability densities during the turns, while the CAT distributions do not. For each distribution, Fig. 12 shows the number of measurements below P_{FA} (probability of false alarm, or probability density noise level) for a range of different values of P_{FA}. It can be seen from Fig. 12 that for P_{FA} below 10^{-7}, the CAT distributions have fewer measurements lower than P_{FA} than the Gaussian distributions. For higher values of P_{FA}, only Gauss4, which was generated specifically from the measurements used, has comparable number of measurements below P_{FA} to the CAT distributions, and that comes at the cost of giving a lower probability density than the CAT distributions during the straight runs.

VI. CAT and Gaussian Distribution Similarities

When the time period between two measurements is long compared to the time scales of vehicle turning maneuvers and the acceleration is relatively small compared to the initial velocity, the CAT distribution is most often a better choice than Gaussian distributions, as was shown in Section V. If we use the same vehicle as in Section III, but have a time period between two measurements that is relatively short compared to the time scales of the vehicle turning maneuvers, the CAT distribution looks like a Gaussian distribution, as shown in Fig. 13, where we have used Δt=1s, and in Fig. 14, where we have kept Δt=10s, but reduced the turn rate to σ_ω=1 deg/s. The CAT distribution also resembles a Gaussian distribution when σ_a times Δt is relatively large compared to the initial velocity, as shown in Fig. 15, where we have kept Δt=10s and σ_ω=5 deg/s but reduced the speed to s_0=10 m/s and the acceleration to σ_a=0.16 m/s^2. In such cases, a Gaussian distribution may be preferred, since it is computationally faster, but if the little extra computational cost can be afforded, the CAT distribution may be used for all cases.

VII. Discussion and Future Work

For association methods that use estimated probability density functions of measurements, accurate association requires that true measurements receive higher pdf values than those of false measurements or measurements of other vehicles. When applied to a simple test scenario with a fairly realistic vehicle trajectory, we found that the proposed CAT distribution gives far higher pdf values for the measurements

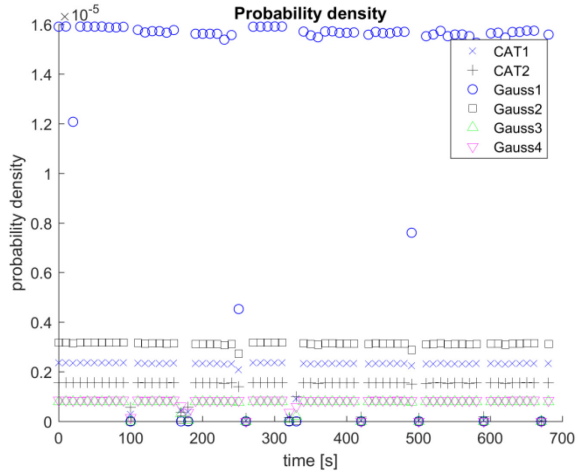

Fig. 9. Probability density of measurements belonging to the vehicle trajectory

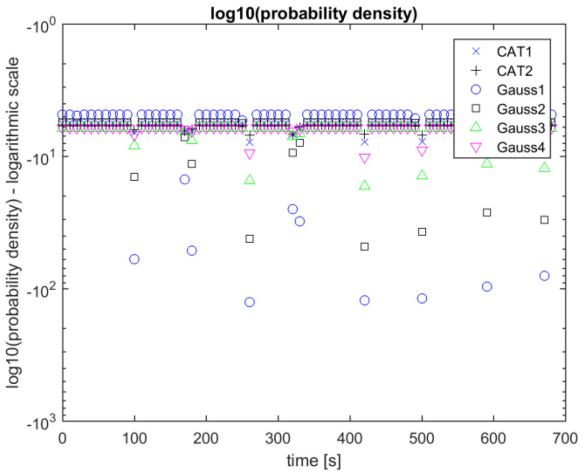

Fig. 11. Log10(probability density) of measurements belonging to the vehicle trajectory, note logarithmic y axis

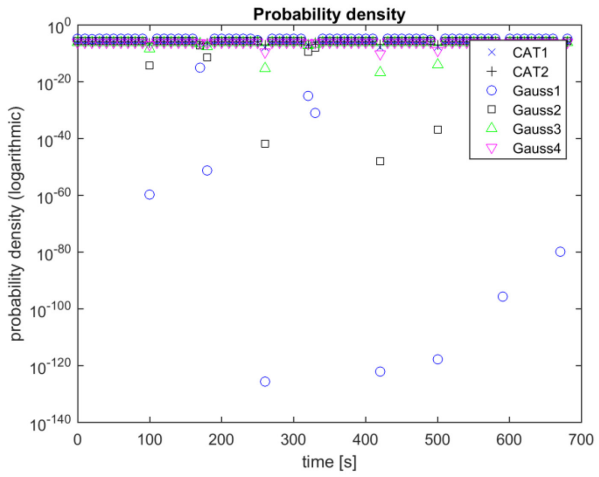

Fig. 10. Probability density of measurements belonging to the vehicle trajectory. Note logarithmic y axis

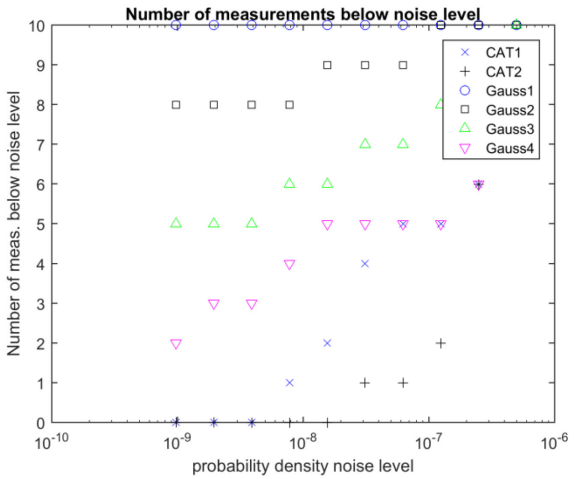

Fig. 12. Number of measurements below P_{FA} at different levels of P_{FA}, note logarithmic x axis

during turns than any of the Gaussian distributions, indicating that using the CAT distribution will allow stable tracking in the presence of far more clutter – or measurements from other vehicles – than using a Gaussian distribution. While Gauss1 yielded significantly higher pdf values during the straight runs than either CAT distribution, it also had by far the worst performance during turns, followed by Gauss2, which only yielded slightly better performance during the straight runs than the CAT distributions. The only two Gaussian distribution to consistently yield pdf values higher than 10^{-20} during turns – compared to about 10^{-6} during straight runs – performed worse than the CAT distribution also during straight runs. As the pdf values during straight runs are generally much higher than during turns, tracking the straight runs will rarely be a problem in the first place, unless tracking the turns is plain hopeless.

If the time period between the initial vehicle position and the measurement is small compared to the time scales of vehicle turning maneuvers, or if σ_a times Δt is relatively large compared to the initial velocity, then a Gaussian distribution gives a good representation of the possible vehicle positions. For large time periods or smaller accelerations, the distribution presented in this paper gives a better representation of the possible vehicle positions. These are only rough guidelines, and part of our future work will be to develop better guidelines for the choice of distribution, based on the vehicle's possible accelerations and turn rates, its initial speed and the time period between the initial vehicle position and the measurement.

The CAT distribution presented in this paper is deduced under the assumption of low uncertainty of both the measurement position and the initial velocity vector. A natural continuation would be to deduce a distribution that also includes the effects of measurement noise and uncertainty of the initial velocity vector.

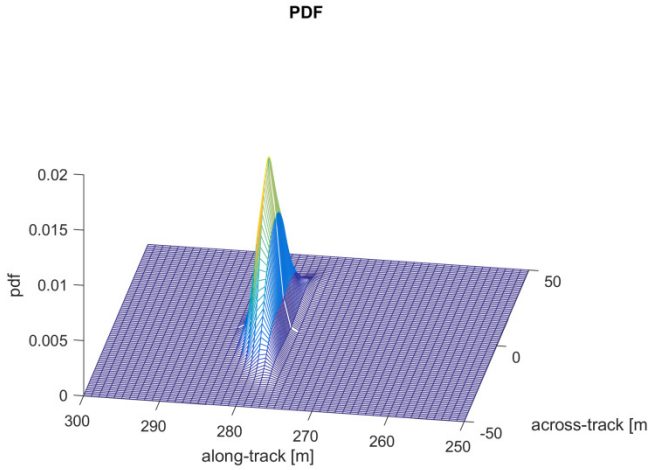

Fig. 13. The CAT distribution for Δt=1s, s_0=280 m/s, σ_a=1.67 m/s^2 and σ_ω=5 deg/s

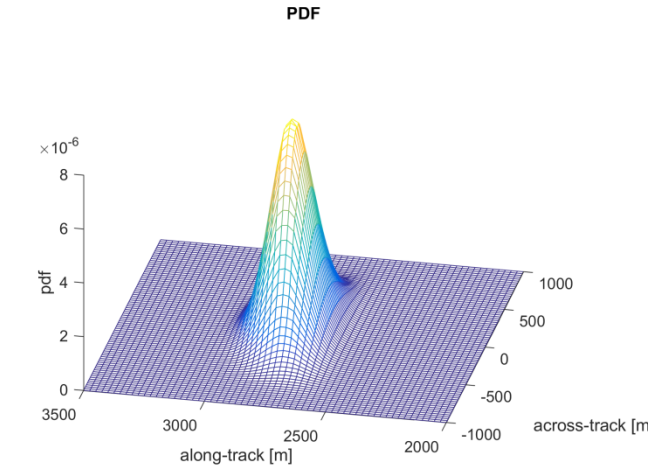

Fig. 14. The CAT distribution for Δt=13s, s_0=280 m/s, σ_a=1.67 m/s^2 and σ_ω=1 deg/s

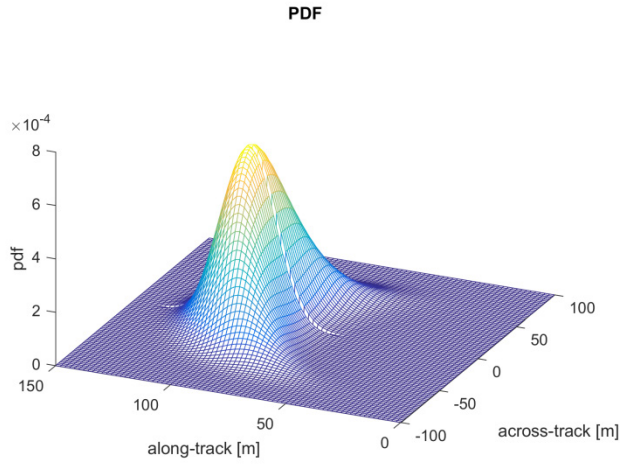

Fig. 15. The CAT distribution for Δt=10s, s_0=10 m/s, σ_a=0.16 m/s^2 and σ_ω=5 deg/s

REFERENCES

[1] Y. Bar-Shalom, P. K. Willett and X.Tian, "Tracking and data fusion, a handbook of algorithms", YBS Publishing, CT, USA, 2011.

[2] P. Mahalanobis, "On tests and measures of group divergence I. Theoretical formulae" J. and Proc. Asiat. Soc. of Bengal , 26, pp. 541–588, 1930.

[3] D.B. Reid, "An algorithm for tracking multiple targets," IEEE Trans. on Automatic Control, vol. 24, no. 6, pp. 843-854, Dec. 1979.

[4] Xuezhi Wang, S. Challa and R. Evans, "Gating Techniques for Maneuvering Target Tracking in Clutter", IEEE Trans. On Aerospace and Electronic Systems, vol 38, pp. 1087-1097, Dec. 2002.

[5] T. Bailey, B. Upcroft, H. F. Durrant-Whyte, "Validation gating for non-linear, non-Gaussian target tracking", 2006 9th International Conference on Information Fusion, IEEE, 2006.

[6] B. Gade, M. Kloster and M. Aronsen, "Non-elliptical validation gate for maritime target tracking", 2018 21st International Conference on Information Fusion, IEEE, 2018.

[7] A. W. Long, K. C. Wolfe and G. S. Chirikjian, "The Banana Distribution is Gaussian: A Localization Study with Exponential Coordinates", Robotics: Science and Systems VIII, MIT Press, MA, USA, 2013.

[8] S. Thrun, D. Fox and W. Burgard, "A real-time algorithm for mobile robot mapping with applications to multi-robot and 3D mapping", Proceedings of the IEEE International Conference on Robotics and Automation (ICRA'00), San Fransisco, CA, USA, 2000, pp. 321-328.

[9] S. Thrun, "Probabilistic Robotics" MIT Press, MA, USA, 2005.

[10] K. Gade, "A Non-singular Horizontal Position Representation", The Journal of Navigation, Volume 63, Issue 03, pp 395-417, July 2010.

APPENDIX

A. Finding geographical position from acceleration and turn rate

The speed $s(t)$ and course change $\varphi(t)$ at any given moment t between t_0 and $t_0+\Delta t$ are given by

$$s(t)=s_0+at \tag{7}$$

and

$$\phi(t)=\omega t \tag{8}$$

The velocity vector decomposed in the x,y coordinate system is

$$v(t) = \begin{bmatrix} v_x(t) \\ v_y(t) \end{bmatrix} = \begin{bmatrix} s(t)\sin\big(\varphi(t)\big) \\ s(t)\cos\big(\varphi(t)\big) \end{bmatrix} \tag{9}$$

By inserting (7) and (8) and integrating, the position vector is found to be

$$\begin{bmatrix} x(\Delta t) \\ y(\Delta t) \end{bmatrix} = \begin{bmatrix} s_0 \int_0^{\Delta t}(\sin(\omega \cdot t))dt + a\int_0^{\Delta t}(t\sin(\omega \cdot t))dt \\ s_0 \int_0^{\Delta t}(\cos(\omega \cdot t))dt + a\int_0^{\Delta t}(t\cos(\omega \cdot t))dt \end{bmatrix} \tag{10}$$

By solving the integrals, the full position vector equation is found to be

$$\begin{bmatrix} x(\Delta t) \\ y(\Delta t) \end{bmatrix} = \begin{bmatrix} s_0\left(-\frac{c}{\omega}+\frac{1}{\omega}\right) + a\left(\frac{s}{\omega^2}-\frac{\Delta tc}{\omega}\right) \\ \frac{1}{\omega}s_0 s + a\left(\frac{c}{\omega^2}+\frac{\Delta ts}{\omega}-\frac{1}{\omega^2}\right) \end{bmatrix} \tag{11}$$

where $s = \sin(\omega\cdot\Delta t)$ and $c = \cos(\omega\cdot\Delta t)$.

B. Finding acceleration and turn rate from geographical position

We have not found closed-form equations for the acceleration and turn rate as functions of the geographical position. Instead, we first find a coarse estimate of the acceleration and turn rate, by using the equations in Appendix B.1. Next, we iterate the procedure in Appendix B.2 to find a good enough estimate of the acceleration and turn rate:

1) Coarse estimates of the acceleration and turn rate

Two different equations for the acceleration can be found from the x- and the y- part of (11):

$$a = \frac{\left(x\omega^2 - s_0\omega(-c+1)\right)}{(s-\omega\Delta tc)} \tag{12}$$

$$a = \frac{\omega^2 y - s_0\omega s}{(c+\omega\Delta ts-1)} \tag{13}$$

A coarse estimate of turn rate may be found from

$$\omega(\Delta t)\approx(2/\Delta t)\cdot\mathrm{atan2}(x,y) \tag{14}$$

Where atan2(y,x) is the four quadrant arctangent of the elements of x and y, and $-\pi <= \mathrm{atan2}(y,x) <= \pi$.

By inserting the coarse estimate of the turn rate from (14) into (12) or (13), we get a coarse estimate of the acceleration.

2) Iteration to find acceleration and turn rate

1. The estimates of the acceleration $a_{est,i}$ and turn rate $\omega_{est,i}$ are used to calculate the corresponding geographical position $x_{est,i}$ and $y_{est,i}$ by using (11).
2. The next (and better) estimates of acceleration and turn rate are found from

$$\begin{bmatrix} a_{est,i+1} \\ \omega_{est,i+1} \end{bmatrix} = \begin{bmatrix} a_{est,i} \\ \omega_{est,i} \end{bmatrix} - \boldsymbol{J^{-1}} \begin{bmatrix} x_{est,i} - x \\ y_{est,i} - y \end{bmatrix}, \tag{15}$$

where $\boldsymbol{J}$ is the Jacobi matrix from (3); this is the generalization of Newton's method for a system of equations.

C. The Jacobi matrix

The elements of the Jacobi matrix can be found to be, by partial derivation of the elements of (11) :

$$\frac{\partial x}{\partial a} = \frac{s}{\omega^2} - \frac{\Delta tc}{\omega}, \tag{16}$$

$$\frac{\partial y}{\partial a} = \frac{c}{\omega^2} + \frac{\Delta ts}{\omega} - \frac{1}{\omega^2}, \tag{17}$$

$$\frac{\partial x}{\partial \omega} = \frac{(s_0+a\Delta t)(\omega\Delta ts+c)-s_0}{\omega^2} + a\frac{\omega\Delta tc-2s}{\omega^3} \tag{18}$$

and

$$\frac{\partial y}{\partial \omega} = (s_0 + a\Delta t)\frac{\Delta tc\omega - s}{\omega^2} - a\frac{\Delta ts\omega+2c+2}{\omega^3}. \tag{17}$$